

Using Rare Gas Permeation to Probe Methanol Diffusion near the Glass Transition Temperature

Jesper Matthiesen, R. Scott Smith, and Bruce D. Kay*

*Fundamental Sciences Directorate, Pacific Northwest National Laboratory,
Post Office Box 999, Mail Stop K8-88, Richland, Washington 99352, USA*

(Received 4 August 2009; revised manuscript received 14 October 2009; published 8 December 2009)

The permeation of rare-gas atoms through deeply supercooled metastable liquid methanol films is used to probe the diffusivity. The technique allows for measurement of supercooled liquid mobility at temperatures near the glass transition. The temperature dependence of the diffusivity is well described by a Vogel-Fulcher-Tamman equation. These new measurements and the temperature dependent kinetic parameters obtained from their analysis provide clear evidence that methanol is a fragile liquid near the glass transition.

DOI: 10.1103/PhysRevLett.103.245902

PACS numbers: 66.10.C-, 65.60.+a, 64.70.pm

Glassy or amorphous materials are widespread in both nature and technology [1,2]. Glassy sugars help stabilize proteins to aid the survival of insects under extreme dehydration [3], optical fibers are made of very pure amorphous silica, and the glass in our windows is an engineered amorphous solid we “see” every day. Understanding the formation of a glass through the extraordinary viscous slow down that accompanies the supercooling of a liquid has been called a major current scientific challenge [4].

Several studies have been reported where probe molecules were used to study the translational diffusion of liquid glass formers both in bulk samples [5,6] and in nanoscale films [7,8]. However, these studies have all been performed in good glass formers with slow crystallization kinetics. Similar measurements in glass formers with fast crystallization kinetics like, e.g., methanol and ethanol have not been performed since their fast crystallization inhibits diffusion measurements near T_g with traditional methods. In the case of methanol ($T_g = 103$ K, $T_{\text{Melt}} = 176$ K), translational self-diffusion measurements at atmospheric pressure have been performed in the range from $T = 154$ K to 292 K [9]. We have previously studied deeply supercooled liquid diffusion using both isotopically labeled water [10,11] and binary layers of amorphous methanol and ethanol [12,13]. In those experiments the intermixing rate of the layered films was determined using the molecular desorption rate from the film’s outer layer. However, this method only works for systems where there is an experimentally measurable desorption rate prior to crystallization. Recent studies by Ediger and co-workers have employed isotopically labeled, vapor deposited films to examine self-diffusion in good glass formers using a combination of desorption and depth profiling techniques [14,15].

We probe the translational diffusion of metastable supercooled liquid methanol at temperatures (100–115 K) around its glass transition (103 K) using the permeation of rare-gas atoms through the nanoscale methanol films. The extracted rare-gas diffusion coefficients together with the available literature diffusion data for

methanol self-diffusion are well-fit by a VFT equation. This markedly non-Arrhenius behavior is indicative of collective complex motion on a rugged energy landscape rather than the physical crossing of a single barrier characteristic of a normal liquid above its melting point [2,16].

The experiments were conducted in a previously described UHV system [17], using molecular beam sources for depositing the krypton and methanol onto a graphene covered Pt(111) substrate. Both were deposited at normal incidence at 25 K. The graphene layer was used to prevent any dissociative interactions between methanol and Pt(111) and was created by standard methods [18]. One monolayer of Kr was deposited onto the graphene substrate and then capped with methanol layers of varying thickness. At 25 K, methanol is deposited as an amorphous nonporous solid which was confirmed by reflection absorption infrared spectroscopy (RAIRS) and rare-gas adsorption [19]. The desorption of Kr from the methanol overlayer was measured with a line-of-sight quadrupole mass spectrometer.

The diffusion rates were obtained using a one-dimensional diffusion model in which Kr diffusion was represented by a series of discrete hops between potential minima between adjacent methanol layers. A set of coupled ordinary differential equations described the hopping of Kr between adjacent minima and we assumed an Arrhenius temperature dependence for the hopping rate [20].

Experiments were conducted with 1 ML of Kr capped by methanol overlayers varying from 50 to 600 ML in thickness and ramp rates from 0.001 to 1.5 K/s. A subset of these experiments are displayed in Fig. 1. Figure 1(a) shows a set of Kr temperature programmed desorption (TPD) traces for a sequence of methanol cap layers from 50 to 400 ML and a ramp rate of 0.6 K/s. In Fig. 1(b) a series of Kr TPD traces are shown for which the methanol cap layer thickness was kept fixed at 100 ML and the TPD rate was varied from 0.001 to 0.6 K/s. In Fig. 1(b) the desorption rate is divided by the ramp rate to normalize the

data. The data show that with increasing overlayer thickness [Fig. 1(a)] or increasing ramp rate [Fig. 1(b)] the Kr desorption is shifted to higher temperatures and the line shape broadens. This is the expected behavior for diffuselike transport through an overlayer. Isothermal experiments (data not shown) confirm that the desorption time scales as L^2 in accordance with diffusive transport and that the extracted diffusivities are in agreement with those derived from the temperature ramped experiments.

The experimental data span the temperature range from about 100 to 115 K. The upper temperature is limited by crystallization of the methanol film that occurs just above 115 K. When the film crystallizes, transport through the film stops and Kr remains trapped in the overlayer until the entire film desorbs at higher temperature (>130 K). The correlation of the temperature at which trapping occurs and crystallization of the methanol was confirmed with RAIRS. The cessation of Kr transport in the crystalline film supports the concept that the rate of gas diffusion is directly related to the diffusivity of the supercooled liquid.

Direct evidence for the correlation between Kr permeation and the supercooled liquid mobility comes from experiments using isotopically labeled methanol layers.

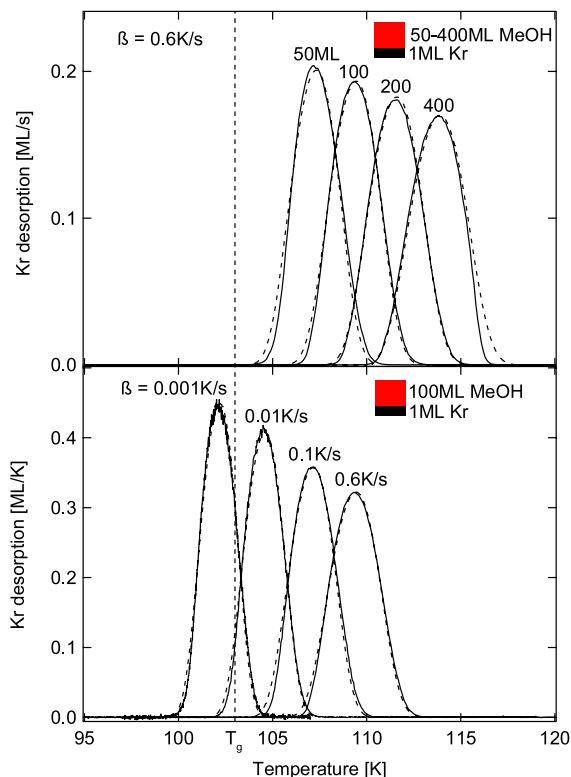


FIG. 1 (color online). (a) The Kr TPD spectra from 1 ML of Kr capped with 50 to 400 ML of methanol (solid lines) and a ramp rate of 0.6 K/s. (b) The Kr TPD spectra from 1 ML of Kr capped with 100 ML of methanol acquired at ramp rates from 0.001 to 0.6 K/s (solid lines). The dashed lines in both (a) and (b) are fits to the Kr TPD spectra made using a one-dimensional diffusion model with an Arrhenius temperature dependence for the diffusivity. The fit parameters are displayed in Fig. 3.

The CO vibrational stretch for the two isotopes occurs at distinct frequencies of 1045 cm^{-1} and 989 cm^{-1} for pure CH_3OH and CD_3OH , respectively. The exact peak position is sensitive to the local molecular environment and is thus a measure of the extent of intermixing of the layers. The inset in Fig. 2 displays time resolved RAIRS spectra of the CO stretch region of CD_3OH for an initially unmixed film of 100 ML of CD_3OH deposited on top of 100 ML of CH_3OH that is heated at a ramp rate of 0.2 K/s. The initial spectrum is at ~ 104 K and is nearly identical to that for a pure CD_3OH film. Subsequent spectra show that the peak red shifts and decreases in intensity with increasing temperature. The final spectrum (~ 111 K) is nearly identical to that of a completely premixed $\text{CH}_3\text{OH}/\text{CD}_3\text{OH}$ film. The spectra have an isosbestic point (a point where they all cross) near 986 cm^{-1} which indicates that the absorbance at any point is due to a linear contribution from two species or states. Therefore, from a vertical cut through the spectra the extent of intermixing can be determined. The extent of mixing calculated from this cut is plotted in Fig. 2 (open squares) along with a simulation (line). Also displayed in Fig. 2 are the Kr permeation data (open circles) obtained during the experiment described above along with its simulation (line). The intermixing of the methanol and the permeation of Kr are clearly occurring over the same temperature range. Both experiments are in excellent agreement with their respective simulations. The diffusivity parameters for the two simulations (see VFT fit in Fig. 4) were the same except that the prefactor for the permeation of Kr was 5 times faster than the diffusivity of the supercooled liquid methanol. Despite this difference the Kr and methanol exhibit similar diffusivity temperature

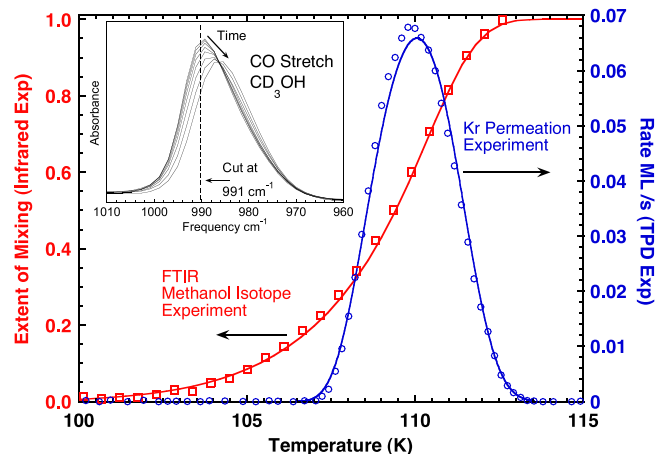


FIG. 2 (color online). The extent of mixing data (squares, left axis) and Kr permeation data (circles, right axis) from a film of 100 ML of CD_3OH deposited on top of 100 ML of CH_3OH that is heated at a ramp rate of 0.2 K/s. The lines are simulations using the VFT parameters from a fit to the Kr permeation data in Fig. 4, except that the prefactor for the extent of intermixing is 0.2 times the prefactor for Kr permeation. Inset: Time resolved FTIR spectra of the CO stretch region of CD_3OH for the film. The spectra span the temperature range from ~ 104 to 110 K in about 1 K increments.

dependences, namely, $D(T)_{\text{Kr}} = \sim 5D(T)_{\text{MeOH}}$. These data provide direct evidence for the quantitative correlation between Kr permeation and the supercooled liquid mobility.

The experimental Kr TPD traces shown in Fig. 1 were fit using the one-dimensional diffusion model (dashed lines). For each TPD spectrum, a set of diffusion Arrhenius parameters (prefactor and activation energy) were used to simulate the Kr TPD spectrum. Figure 3 displays the diffusion Arrhenius parameters that best fit the experimental TPD spectra plotted versus the desorption peak temperature. In the fitting process, the Arrhenius parameters were varied until simulations of the quality displayed in Fig. 1 (dashed lines) were obtained for each individual TPD experiment. The best parameters were those that minimized the chi-square error between the experiment and simulation. Equally good fits were obtained for a range of activation energies and prefactors indicated by the error bars in Fig. 3. The error corresponds to about $\pm 5\%$ in the activation energy and a factor of roughly $10^{\pm 1.5}$ in the prefactor. This range of values corresponds to about a $\pm 4\%$ variation in the diffusion coefficient at the peak desorption temperature. Note that while a single set of Arrhenius parameters can accurately simulate an individual experiment, no single set of Arrhenius parameters can fit the entire set of experiments. The plot in Fig. 3 shows that both the activation energy and prefactor display a smooth monotonic decrease in value with increasing peak temperature. There are compensation effects between the Arrhenius parameters and the inset in Fig. 3 shows a strong linear correlation between the best-fit activation energy and the log of the corresponding best-fit prefactor.

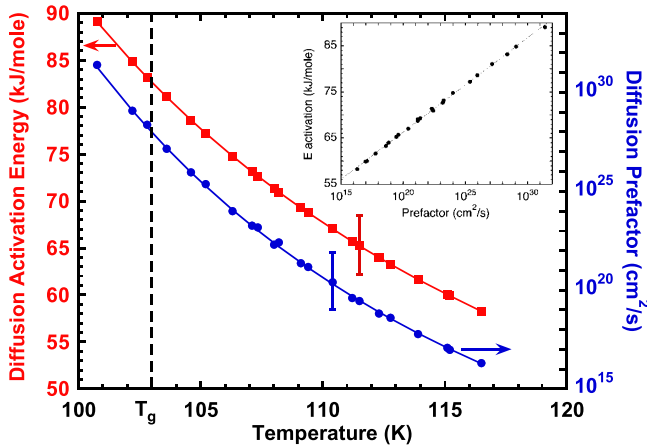


FIG. 3 (color online). The Arrhenius activation energies (solid circles) and prefactors (solid squares) that best fit the experimental Kr desorption spectra plotted versus the desorption peak temperature. The representative error bars correspond to about $\pm 5\%$ in the activation energy and a factor of $10^{\pm 1.5}$ in the prefactor. The solid lines are Arrhenius parameters calculated from the tangent of the VFT curve for Kr diffusion in the inset in Fig. 4. Inset: A plot of the best-fit activation energy versus the log of the corresponding best-fit prefactor.

The main point is that with decreasing temperature there is a marked increase in both the apparent diffusion activation barrier and prefactor. This behavior is reminiscent of the diffusivity of a fragile liquid approaching the glass transition temperature. The solid lines in Fig. 3 are the Arrhenius parameters calculated from the tangent to the Vogel-Fulcher-Tamman (VFT) equation shown below in Fig. 4. Also, the prefactors and activation energies needed to fit the experimental data are unusually large which is another characteristic of a fragile liquid.

Figure 4 is an Arrhenius plot of the Kr diffusivity at the desorption peak temperature for each TPD experiment (solid triangles) along with the methanol self-diffusion data around the melting temperature [9] (solid circles). The error in the best-fit simulated spectra corresponds to an uncertainty in the diffusivity of about $\pm 4\%$, which is smaller than the symbols in Fig. 4. The combined data sets span the temperature range from ~ 100 to 292 K and diffusivities from $\sim 10^{-15}$ to 10^{-5} cm^2/s . The solid black line is a fit of the low temperature Kr permeation data to the VFT equation, $D = D_0 \exp(B/(T - T_0))$ where D is the diffusivity and D_0 , B , and T_0 are fit parameters. The obtained fit parameters for the Kr diffusion alone are $D_0 = 24.1 \text{ cm}^2/\text{s}$, $B = 1320 \text{ K}$, and $T_0 = 65.3 \text{ K}$. Simulations

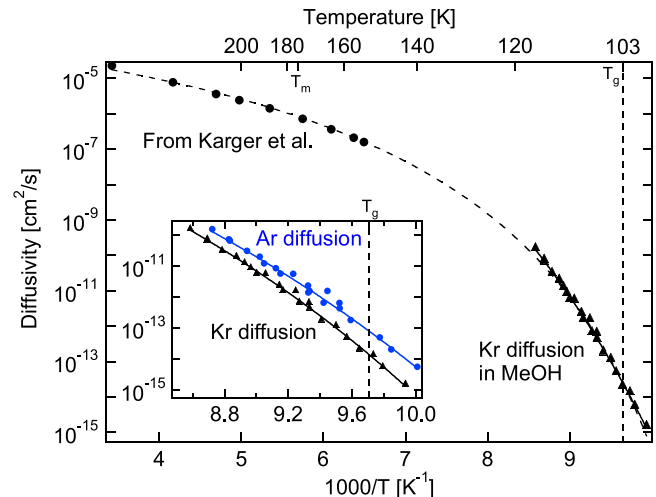


FIG. 4 (color online). An Arrhenius plot of the Kr diffusion in low temperature supercooled methanol (black triangles) and the methanol self-diffusion data from Karger *et al.* [9] (black circles). The solid black line is a fit of the low temperature Kr permeation data to a VFT equation, $D = D_0 \exp(-B/(T - T_0))$. The obtained fit parameters for Kr diffusion alone are $D_0 = 24.1 \text{ cm}^2/\text{s}$, $B = 1320 \text{ K}$, and $T_0 = 65.3 \text{ K}$. The dashed black line is a VFT fit to both the low temperature Kr permeation data and the high temperature methanol self-diffusion data. The obtained parameters for the fit to both data sets are $D_0 = 2.11 \times 10^{-4} \text{ cm}^2/\text{s}$, $B = 525.7 \text{ K}$, and $T_0 = 80.6 \text{ K}$. Inset: An expanded scale showing the Kr (solid triangles) and Ar (solid circles) diffusion coefficients in methanol. The solid lines are VFT fits to only the low temperature diffusion data. The fit parameters for Kr diffusion are given above and the fit parameters for Ar are $D_0 = 14.1 \text{ cm}^2/\text{s}$, $B = 1313 \text{ K}$, and $T_0 = 62.9 \text{ K}$.

using this single set of VFT parameters (solid line) are in excellent agreement with all of the experimental TPD spectra. This is in contrast to an Arrhenius function where each experiment was fit with a different set of Arrhenius parameters (see Fig. 3). The success of the Arrhenius function to fit an individual TPD spectrum is due to the steep temperature dependence of the diffusivity (high activation energy) and as a result most of the diffusion occurs in a narrow temperature region near the desorption peak.

The dashed black line in Fig. 4 is a VFT fit to both the low temperature Kr permeation data and the high temperature methanol self-diffusivity data. The obtained parameters for the fit to the combined data sets are $D_0 = 2.11 \times 10^{-4} \text{ cm}^2/\text{s}$, $B = 525.7 \text{ K}$, and $T_0 = 80.6 \text{ K}$. While this VFT curve is slightly different than the VFT fit to the low temperature data alone (solid line), simulations using these VFT parameters also give reasonably good fits to the experimental data. The overall point is that both sets of data can be connected by a single VFT curve. The VFT fit corroborates the continuity between the liquid and deeply supercooled liquid data and demonstrates the rapid increase in the apparent diffusion activation barrier at temperatures approaching T_g .

Experiments using Ar were also conducted. The extracted diffusion coefficients for both Ar, along with those already presented for Kr, are shown in the inset of Fig. 4. The data sets have very similar temperature dependences that are both well fit by VFT functions (solid lines) that are slightly offset. The Ar diffusivity is about a factor of 4 faster than Kr over the measured range. A small difference in diffusion rate might be expected due to differences in van der Waals radius and mass but these effects are not large enough to account for a factor of 4. For example, in liquid water under ambient conditions Ar diffusion is only about 20% faster than Kr. The significant differences in diffusivity for various rare gases is a sensitive probe of the dynamically heterogeneous nature of the fragile supercooled methanol [21–24] and will be discussed in a future publication. Despite the factor of 4 difference in diffusivity at temperatures near T_g , when compared to the overall dynamic range of the diffusivity the difference is relatively small.

It is interesting to compare the kinetic parameters for diffusion in the normal liquid and in deeply supercooled liquid methanol. The apparent activation energy changes from 12.0 to 81.2 kJ/mol, i.e., by almost a factor of 7, whereas the prefactor changes from $3.2 \times 10^{-3} \text{ cm}^2/\text{s}$ to $\sim 10^{27} \text{ cm}^2/\text{s}$, i.e., by a factor of $\sim 10^{30}$ as the temperature decreases from 292 to 100 K. This very clearly shows the non-Arrhenius temperature dependence of the diffusivity. The low temperature diffusion prefactors and activation energies are unusually high. For example, a normal liquid diffusion prefactor is $\sim 10^{-2} \text{ cm}^2/\text{s}$ which corresponds to an attempt frequency of $\sim 10^{13} \text{ s}^{-1}$, whereas the prefactor needed to fit the Kr TPD spectrum from the 200 ML film in

Fig. 1(a) is $\sim 10^{19} \text{ cm}^2/\text{s}$, which naively corresponds to an attempt frequency of 10^{34} s^{-1} . Obviously, such a prefactor is unphysically large for a single barrier crossing event and thus provides evidence of multimolecular, cooperative motion as being required for diffusion near T_g . Furthermore, the apparent diffusion activation energy, 81.2 kJ/mole, exceeds the vaporization energy, 41.8 kJ/mole, of the supercooled liquid [13].

The combined experimental data and the numerical simulations above show that rare-gas atoms permeating through a nanoscale supercooled liquid film provide an excellent method to probe mobility near the glass transition. Temperature dependent diffusivity data as presented here, especially near T_g , are requisite to address many of the questions related to supercooled liquids and amorphous materials.

This work was supported by the U.S. Department of Energy Office of Basic Energy Sciences, Division of Chemical Sciences, Geosciences, and Biosciences. The research was performed using EMSL, a national scientific user facility sponsored by DOE's Office of Biological and Environmental Research and located at PNNL, which is operated for DOE by Battelle.

*Corresponding author.

- [1] C. A. Angell *et al.*, J. Appl. Phys. **88**, 3113 (2000).
- [2] P. G. Debenedetti and F. H. Stillinger, Nature (London) **410**, 259 (2001).
- [3] J. H. Crowe, J. F. Carpenter, and L. M. Crowe, Annu. Rev. Physiol. **60**, 73 (1998).
- [4] P. W. Anderson, Science **267**, 1615 (1995).
- [5] F. R. Blackburn, C. Y. Wang, and M. D. Ediger, J. Phys. Chem. **100**, 18249 (1996).
- [6] M. T. Cicerone and M. D. Ediger, J. Chem. Phys. **104**, 7210 (1996).
- [7] R. C. Bell *et al.*, J. Am. Chem. Soc. **125**, 5176 (2003).
- [8] R. C. Bell *et al.*, J. Chem. Phys. **127**, 024704 (2007).
- [9] N. Karger, T. Vardag, and H. D. Ludemann, J. Chem. Phys. **93**, 3437 (1990).
- [10] R. S. Smith *et al.*, Chem. Phys. **258**, 291 (2000).
- [11] R. S. Smith and B. D. Kay, Nature (London) **398**, 788 (1999).
- [12] P. Ayotte *et al.*, Phys. Rev. Lett. **88**, 245505 (2002).
- [13] R. S. Smith, P. Ayotte, and B. D. Kay, J. Chem. Phys. **127**, 244705 (2007).
- [14] S. F. Swallen *et al.*, J. Phys. Chem. B **113**, 4600 (2009).
- [15] S. F. Swallen *et al.*, Phys. Rev. Lett. **102**, 065503 (2009).
- [16] F. H. Stillinger, Science **267**, 1935 (1995).
- [17] T. Zubkov *et al.*, J. Chem. Phys. **127**, 184707 (2007).
- [18] B. Lang, Surf. Sci. **53**, 317 (1975).
- [19] K. P. Stevenson *et al.*, Science **283**, 1505 (1999).
- [20] J. L. Daschbach *et al.*, Phys. Rev. Lett. **92**, 198306 (2004).
- [21] C. Donati *et al.*, Phys. Rev. Lett. **80**, 2338 (1998).
- [22] C. Donati *et al.*, Phys. Rev. E **60**, 3107 (1999).
- [23] W. Kob *et al.*, Phys. Rev. Lett. **79**, 2827 (1997).
- [24] M. D. Ediger, Annu. Rev. Phys. Chem. **51**, 99 (2000).